

Design of Spacecraft Formation Orbits Relative to a Stabilized Trajectory

F.Y. Hsiao* and D.J. Scheeres†
Department of Aerospace Engineering
The University of Michigan
Ann Arbor, MI 48109-2140

Abstract

This paper investigates the design of spacecraft formation orbits traveling relative to a general trajectory. To describe the motion we approximate the time-varying linear dynamics about the trajectory with a locally time-invariant system and use linear orbit elements to describe the relative trajectories. We find sufficient conditions under which the relative motion is stable and a controller can be designed. We consider the problem of specifying the orientation of the fundamental orbits, which is equivalent to eigenvector placement, and show how these modes can be combined to force the formation to fly in a range of orientations. Applications of our approach to relative motion in rotating and non-rotating systems are given.

INTRODUCTION

A general control law to stabilize the relative motion about a general trajectory in a Hamiltonian system and related methods of relative trajectory design are studied in this paper. Among the possible applications of this work is formation flight about a halo orbit in the Hill three body problem, an unstable periodic orbit in the vicinity of libration points in the Sun-Earth system. This work is motivated by potential future applications of spacecraft formation flight for interferometric imaging of distant stellar systems. Flying formations of spacecraft in the vicinity of L_2 halo orbits has been recognized as a feasible environment for this application. Results of this study will contribute to the possible application of formation flight techniques in this unstable environment.

The idea for using the center manifold of a halo orbit for formation flight was proposed in Ref. [1]. However, the utilization of the center manifold of an unstable orbit for formation flight is constrained by its long frequency of relative motion and the difficulty in control and computation of the orbits. The current state of the art for the computation and control of motion in an unstable halo orbit center manifold is reviewed in Ref. [2, 3] and indicates that highly precise computation must be made in order to keep the trajectory from diverging. The technique we propose here eliminates both of these concerns, as we are able to generate relative trajectories with shorter periods, and by stabilizing the relative motion relieve many of the concerns about controlling and computing the relative motions over longer spans of time. Our current approach to the design and control of formation flight trajectories should be distinguished from previous work, such as that reported in Refs. [4–6], as those efforts focus on the control and design of formation flight in near-Earth orbits.

*Ph.D. Candidate; email: fhsiao@umich.edu; TEL: (734) 764-7573

†Associate Professor of Aerospace Engineering; Senior Member AIAA; email: scheeres@umich.edu; TEL: (734) 615-3282; FAX: (734) 763-0578

The current work in this paper is an extension of the work reported in Ref. [10] that investigated the feasibility of the “local time” algorithm for the description of relative motion about a halo orbit. Here we investigate the general rule from which different controllers are designed to stabilize the relative motion. We also investigate different approaches to design relative trajectories for application to various space missions. The goal of this analysis is to come up with a general control law which allows formation flight dynamics to be arbitrarily assigned. The ultimate goal of this work is to develop efficient approaches to the implementation of distributed interferometric imaging by relying on the motion of spacecraft relative to each other to cover the necessary elements of the “image plane” that the imaging system is trying to reconstruct [7]. Our approach will be used in conjunction with innovative interferometric imaging approaches that can relieve the tight relative position control constraints that previous system concepts have had to deal with. Thus, by defining the preferred planes of motion for our stabilized system we define the preferred imaging surfaces as a function of time.

In detail, our paper covers the following items. First we find a condition under which the relative motion about a general trajectory in a celestial system is stabilized. Then we apply our algorithm to the relative motions about a halo orbit in the Hill three body problem. The control law creates a linear, time varying system about the periodic orbit, where all motion winds on tori about the periodic orbit. It can be shown that these orbits are stable over both short and long periods of time, and that their winding number about the periodic orbit can be controlled by the gain of the feedback law and can be made arbitrarily large. Then, in order to better study the resulting dynamics of our stabilized system, we introduce a “short time” approximation, which allows us to characterize relative motion with a simpler, time-invariant linear system. With this approximation, we also evaluate the control cost over a whole period and show that it is feasible. Finally, based on the concept of “linear orbit elements” that relates the geometric description of relative motion along a periodic orbit to the eigenstructures of the dynamics matrix, we come up with several algorithms for trajectory design. By studying the techniques of eigenstructure assignment we can better understand how our system can be used for interferometric imaging applications.

MODEL OF SPACECRAFT MOTION

Equations of Motion

To deal with the formation flight of spacecraft, we can view it as a constellation of spacecrafts flying in the vicinity of a spacecraft in the nominal trajectory in a specific celestial circumstance. Assume the triad (x, y, z) are the coordinates in the body fixed frame of the first spacecraft, and this frame is rotating about the z axis with rotation rate ω . The force potential in this circumstance is defined as $U(\mathbf{r})$. According to dynamics we can write the equations of motion as:

$$\begin{aligned} \ddot{\mathbf{r}}_I &= \frac{\partial U(\mathbf{r})}{\partial \mathbf{r}} \\ (1) \quad &= \ddot{\mathbf{r}}_b + \dot{\omega} \times \mathbf{r} + 2\omega \times \dot{\mathbf{r}} + \omega \times (\omega \times \mathbf{r}) \end{aligned}$$

where $\mathbf{r} = \sqrt{x^2 + y^2 + z^2} \hat{r}$. Assume ω is constant. Eq. (1) can be expressed as:

$$(2) \quad \ddot{x} - 2\omega \dot{y} = \frac{\partial V}{\partial x}$$

$$(3) \quad \ddot{y} + 2\omega \dot{x} = \frac{\partial V}{\partial y}$$

$$(4) \quad \ddot{z} = \frac{\partial V}{\partial z}$$

$$(5) \quad V = U(\mathbf{r}) + \frac{1}{2}\omega^2(x^2 + y^2)$$

Although Eqs. (2)–(4) are derived from dynamics in a body fixed frame in a specific circumstance, we can view ω as a free parameter and V as an arbitrary force potential so that all space missions satisfying

these equations of motion can be analyzed. In fact, if ω is taken to be zero, the above equations of motion degenerate to those in an inertial frame.

The Hill Problem

A spacecraft's trajectory in the vicinity of a Halo orbit in Sun-Earth system is highly unstable and non-Keplerian. To compute the non-linear equations of motion, we use an approximation to the restricted three-body problem, known as the Hill problem⁸. The three dimensional motion is governed by the equations of motion which have the same structure as Eqs. (2)–(4), where the x axis points towards Earth from the Sun, the z axis points normal to the Earth orbital plane and the y axis completes the triad. In this problem, ω is the rotation rate of the Earth's orbit about the Sun and the force potential is taken as

$$(6) \quad V = \frac{\mu}{r} + \frac{1}{2}\omega^2(3x^2 - z^2)$$

where μ is the gravitational parameter of the Earth. The Lagrange equilibrium points have the coordinates $(\pm(\frac{\mu}{3\omega^2})^{1/3}, 0, 0)$ ⁸ in this system.

The Hill Equations have been numerically integrated with proper initial conditions to find a periodic halo orbit, similar to the Genesis halo orbit during its main mission phase². The period of this orbit is 179 days. It has two pairs of stable oscillation modes, one with the same period as that of the rotating frame leading to unity eigenvalues, with the other slightly longer leading to a pair of eigenvalues on the unit circle, and one pair of characteristic exponents $\sigma = \pm 4.757 \times 10^{-7}/s$ (a characteristic time of 24.3 days), one of which causes a hyperbolic instability.

Linearized Dynamics

To derive equations for relative motion between the spacecraft, we assume the second spacecraft is on a non-periodic orbit in the vicinity of the first spacecraft. Assume the first spacecraft has a trajectory defined as $\mathbf{R}(t; \mathbf{R}_o, \mathbf{V}_o)$ with the property, $\mathbf{R}(t+T) = \mathbf{R}(t)$, where T is the period. Naturally, the velocity, $\mathbf{V}(t; \mathbf{R}_o, \mathbf{V}_o)$, is also periodic. Similarly, we can define the position and velocity vectors for the second spacecraft by $\mathbf{r}(t; \mathbf{r}_o, \mathbf{v}_o)$ and $\mathbf{v}(t; \mathbf{r}_o, \mathbf{v}_o)$. Since the second spacecraft is initially in the vicinity of the first spacecraft, linear systems theory can be applied to describe their relative dynamics. We define $\mathbf{X} = [\mathbf{R}; \mathbf{V}]$, $\mathbf{x} = [\mathbf{r}; \mathbf{v}]$, and $\delta\mathbf{x}$ as the difference between them, then the dynamics of $\delta\mathbf{x}$ can be approximated by:

$$(7) \quad \delta\mathbf{x} = \mathbf{x} - \mathbf{X}$$

$$(8) \quad \delta\dot{\mathbf{x}} = A(t)\delta\mathbf{x}$$

$$(9) \quad A(t) = \frac{\partial \mathbf{F}}{\partial \mathbf{X}}$$

$$(10) \quad A(t+T) = A(t)$$

where \mathbf{F} is the dynamics function corresponding to Eqs. (2)-(4). The solution for relative motion can be expressed as:

$$(11) \quad \delta\mathbf{x} = \Phi(t, t_o)\delta\mathbf{x}_o$$

$$(12) \quad \Phi(t, t_o) = \frac{\partial \mathbf{X}(t; \mathbf{X}_o)}{\partial \mathbf{X}_o}$$

$$(13) \quad \dot{\Phi}(t, t_o) = A(t)\Phi(t, t_o)$$

$$(14) \quad A(t) = \left[\begin{array}{c|c} 0 & I_{3 \times 3} \\ \hline V_{\mathbf{r}\mathbf{r}} & 2\omega J \end{array} \right]$$

$$(15) \quad J = \begin{bmatrix} 0 & 1 & 0 \\ -1 & 0 & 0 \\ 0 & 0 & 0 \end{bmatrix}$$

$$(16) \quad \Phi(t_o, t_o) = I_{6 \times 6}$$

where Φ is the state transition matrix (STM), and $\delta \mathbf{x}_o$ is the initial offset from the first spacecraft, i.e., the periodic orbit.

STABILIZING THE RELATIVE MOTION

In Ref. [9], the dynamics of long and short time spans for this relative motion are discussed more fully. In Ref. [10], we see that the relative motion of the spacecraft over a short time span centered at t_i can be understood by analyzing the eigenvalues and eigenvectors of the matrix $A(t_i)$. Therefore, in deriving our control law we will use these “short-term” dynamics to guide our thinking.

The goal of our investigation is to stabilize relative motions in the sense of Lyapunov (not asymptotic stability). According to Ref. [11], Lyapunov stability is defined as following:

An equilibrium point x_e of the system $\dot{x} = A(t)x$ is stable in the sense of Lyapunov if for any $\epsilon > 0$, there exists a value $\delta(t_0, \epsilon) > 0$ such that if $\|x(t_0) - x_e\| < \delta$, then $\|x(t) - x_e\| < \epsilon$, regardless of t , where $t > t_0$

In celestial mechanics, the stabilized trajectory will consist of oscillatory motions about the nominal trajectory, which in this context can be interpreted as motions in the center manifold. Now consider Eq. (8) over a short time span centered at $t = t_i$ and expand it.

$$(17) \quad \delta \mathbf{r}'' - 2\omega J \delta \mathbf{r}' - V_{\mathbf{r}\mathbf{r}}(t_i) \delta \mathbf{r} = 0$$

A feedback controller can be designed as

$$(18) \quad \begin{aligned} \mathcal{T}_c &= -V_{cv} \delta \mathbf{r}' - V_{cr} \delta \mathbf{r} \\ &= \mathcal{T}_{cv} \delta \mathbf{r}' + \mathcal{T}_{cr} \delta \mathbf{r} \end{aligned}$$

Then the equations of motion in the feedback system are

$$(19) \quad \delta \mathbf{r}'' - (2\omega J + V_{cv}) \delta \mathbf{r}' - (V_{\mathbf{r}\mathbf{r}} + V_{cr}) \delta \mathbf{r} = 0$$

$$(20) \quad \delta \mathbf{r}'' - S \delta \mathbf{r}' - V \delta \mathbf{r} = 0$$

If V_{cv} and V_{vr} are chosen skew symmetric and symmetric respectively, the Hamiltonian structure is maintained. Namely, S and V in Eq. (20) are skew symmetric and symmetric respectively. Moreover, if we can find a condition under which relative motions are kept in the center manifolds, the controller can then be obtained by simply subtracting the original Coriolis and force potential matrices from the desired ones. This would increase our choice in future orbit design. Therefore, we are concentrating on finding the condition for stability rather than proposing a specific control law.

Assume V in Eq. (20) is negative definite and consider a Lyapunov function $\mathcal{V}(\delta \mathbf{r}, \delta \dot{\mathbf{r}})$,

$$(21) \quad \mathcal{V}(\delta \mathbf{r}, \delta \dot{\mathbf{r}}) = -\frac{1}{2} \delta \mathbf{r}^T V \delta \mathbf{r} + \frac{1}{2} \delta \dot{\mathbf{r}}^T \delta \dot{\mathbf{r}}$$

Then $\mathcal{V}(0) = 0$ and $\mathcal{V}(\mathbf{x}) > 0$ if $\mathbf{x} \neq 0$, where $\mathbf{x} = (\delta \mathbf{r}, \delta \dot{\mathbf{r}})$.

$$(22) \quad \begin{aligned} \dot{\mathcal{V}}(\delta \mathbf{r}, \delta \dot{\mathbf{r}}) &= -\delta \dot{\mathbf{r}}^T V \delta \mathbf{r} + \delta \dot{\mathbf{r}}^T \delta \ddot{\mathbf{r}} \\ &= -\delta \dot{\mathbf{r}}^T V \delta \mathbf{r} + \delta \dot{\mathbf{r}}^T S \delta \dot{\mathbf{r}} + \delta \dot{\mathbf{r}}^T V \delta \mathbf{r} \\ &= \delta \dot{\mathbf{r}}^T S \delta \dot{\mathbf{r}} \\ &= 0 \end{aligned}$$

Since the requirement for Lyapunov stability is that the time derivative of the Lyapunov function is less than or equal to zero, our linear system is proved stable in the sense of Lyapunov. Also, due to a Hamiltonian structure, this result implies that our local time invariant system has all poles on the imaginary axis. Figures 1 and 2 provide two examples of the robustness of the controller developed from the sufficient condition. The controlled trajectory remains stable after two halo orbit periods (about 1 year), while the uncontrolled trajectory diverges after 66 days.

Another important feature in the realizability of our control law is its cost. Here we define cost as the integral of control acceleration over time. Assume the greatest oscillation frequency in the system is ω_{max} , the total cost would be bounded as

$$\begin{aligned}
|\Delta \mathbf{V}| &= \int_0^t |\mathbf{a}| d\tau \\
&= \int_0^t |\mathcal{T}_{cv} \delta \mathbf{r}' + \mathcal{T}_{cr} \delta \mathbf{r}| d\tau \\
&\leq \int_0^t (|\mathcal{T}_{cv} \delta \mathbf{r}'| + |\mathcal{T}_{cr} \delta \mathbf{r}|) d\tau \\
&\leq \int_0^t (\omega_{max} \|\mathcal{T}_{cv}\|_2 + \|\mathcal{T}_{cr}\|_2) |\delta \mathbf{r}| d\tau \\
&\leq \int_0^t (\omega_{max} \|\mathcal{T}_{cv}\|_2 + \|\mathcal{T}_{cr}\|_2) (\omega_{max} \|\Phi_{rv}\|_2 + \|\Phi_{rr}\|_2) |\delta \mathbf{r}_0| d\tau \\
(23) \quad &\leq |\delta \mathbf{r}_0| \left[\int_0^t (\omega_{max} \|\mathcal{T}_{cv}\|_2 + \|\mathcal{T}_{cr}\|_2) (\omega_{max} \|\Phi_{rv}\|_2 + \|\Phi_{rr}\|_2) d\tau \right]
\end{aligned}$$

where $\|\cdot\|_2$ is the 2-norm of a matrix which is usually defined as $\sqrt{\lambda_{max}(AA^T)}$, where λ_{max} denotes the maximum eigenvalue of AA^T . Φ is the state transition matrix, and

$$(24) \quad \Phi(t, 0) = \begin{bmatrix} \Phi_{rr} & \Phi_{rv} \\ \Phi_{vr} & \Phi_{vv} \end{bmatrix}$$

Systems Without Coriolis Force

To simplify our analysis, we first consider a system where the Coriolis force is nulled out. To discuss the stability of this system we take the free parameter, S , as zero, and, obviously, the same result is obtained. That is, an inertial frame has the same sufficient condition for stability. Furthermore, this also implies that we can make an ‘‘artificial inertial environment’’ by nulling out the natural Coriolis force and utilize properties of inertial frame for formation flight. For example, if the force potential is controlled diagonal and negative definite, the relative motions are just harmonic oscillations in three dimensional space. We are able to design a general trajectory by combining these oscillations with particular initial conditions.

In addition to force potential control, we can compute the upper bound of cost in velocity term in Eq. (18) to estimate the extra cost of this control.

$$\begin{aligned}
\mathcal{T}_{vc} &= -V_{cv} \delta \mathbf{r}' \\
&= 2\omega J \delta \mathbf{r}' \\
&\leq 2\omega \|\delta \mathbf{r}'\| \\
&\sim 2k\omega^2 \|\delta \mathbf{r}\| \\
(25) \quad &\sim 0.079k \|\delta \mathbf{r}\| \quad nm/s^2
\end{aligned}$$

where k is the ratio of highest mode frequency to the frame rotation rate. The cost is low enough to implement using a low-thrust engine. The upper limit of the total cost is estimated in Eq. (23) and numerically simulated in Figure 3.

Systems With Coriolis Force

Given V_{cv} zero or skew symmetric and $V_{rr} + V_{cr}$ negative definite, Eq. (19) is proved stable. One example is the feedback control law proposed in Ref. [9]. To implement this control at a given time t_i , we evaluate the

local eigenstructure of the matrix $A(t_i)$, find the characteristic exponents of the hyperbolic motion $\pm\sigma(t_i)$, and find the eigenvectors that define the stable and unstable manifolds of this motion $\mathbf{u}_{\pm}(t_i)$, where the “+” denotes the unstable manifold and “-” denotes the stable one. Then the applied control acceleration is:

$$(26) \quad \mathcal{T}_c = -\sigma(t_i)^2 G [\mathbf{u}(t_i)_+ \mathbf{u}(t_i)_+^T + \mathbf{u}(t_i)_- \mathbf{u}(t_i)_-^T] \delta \mathbf{r}$$

where G is the gain parameter and $\delta \mathbf{r}$ is the measured relative position vector, i.e., the offset between the periodic orbit and the spacecraft at time t_i . This control law maintains the structure of the problem, and provides local and global stability if the gain constant G is chosen sufficiently large. In fact, as shown in Figure 4, after the control law in Eq. (26) was applied, the force potential becomes negative definite. The upper limit of total cost is also estimated in Eq. (23) and numerically simulated in Figure 5. Figure 6 and Figure 7 give two more examples about the stability and cost of this control law.

LINEAR ORBITAL ELEMENTS

Local dynamics formulation

Having found a sufficient condition under which the closed-loop system is stable, we now concern ourselves with the dynamics of the controlled system. In previous sections, we approached the problem by cutting the orbit into several pieces and treating each of segment as time invariant instead of considering the original linearized time varying system over a whole period. If the time interval is sufficiently small, we can understand our system by investigating the eigen-structure of each local $\tilde{A}(t_i)$ (stabilized) matrix. For the case of a completely stable map, there are three pairs of imaginary eigenvalues, known as the modes of the system. The trajectory described by each mode forms an elliptical orbit relative to the nominal trajectory with the origin of the frame at its the center. The actual trajectory is the linear combination of these three modes. Since $\tilde{A}(t_i)$ is not constant over the whole orbit period, we cannot define one set of some constants describing the relative motion over the entire orbit period. Instead, we define a secular set of “Linear Orbital Elements” to describe the geometry of the trajectory.

Classical Orbital Elements

Among the six classical orbital elements defined in Astrodynamics, five of them are sufficient to completely describe the size, shape and orientation of an orbit. The sixth element pinpoints the position of the satellite along the orbit at a particular time. These elements are defined as follows¹²: *the semi-major axis* a , *the eccentricity* e , *the inclination* i , *longitude of the ascending node* Ω , *the argument of periapsis* ω , and *the mean anomaly* M . In traditional astrodynamics the utilization of classical orbital elements provides us with a set of coordinates that allow us to immediately understand the geometry of motion. The same idea can be applied to our controlled trajectory as well, defining a set of geometrically meaningful elements that can be used in the design of relative motion, as illustrated in Figure 8. Thus we would like to develop a set of elements, called “Linear Orbital Elements”, to describe the geometry of the controlled trajectory relative to the periodic halo orbit, as shown in Figure 9. Provided with proper assumptions, each mode generates a slowly varying elliptical orbit relative to the halo orbit. However, there are some fundamental differences between our case and elliptical orbits in two body problem:

1. The length of semi-major axis is not needed. Since these are linear motions, we don’t concern ourselves with their amplitude. Hence, the semi-major axis a , and the eccentricity e are replaced by *the ratio of major-axis to minor-axis* (a/b) to describe the in-plane orbital shape.
2. The origin of this elliptic motion is located at the center of the ellipse instead of at its focus. As a result, the argument of periapsis is replaced by the *in-plane orientation of the major axis* denoted by ψ (since ω represents frequency in this paper).

3. The mean anomaly is not defined in the current application, but could be in future work.

Linear Orbital Elements

Assume the eigenvalue and eigenvector of $A(t_i)$ are $\pm j\omega_k$ and $\mathbf{u}_k = \vec{\alpha}_k \pm \vec{\beta}_k$, where the subscription k denotes each mode. The mathematic descriptions can be obtained by following usual procedures used in Astrodynamics, and are listed as follows ¹⁰.

$$(27) \quad \hat{h}_k = \frac{\vec{\beta}_k \times \vec{\alpha}_k}{|\vec{\beta}_k \times \vec{\alpha}_k|}$$

$$(28) \quad \hat{n}_k = \hat{z} \times \hat{h}_k$$

$$(29) \quad \left(\frac{a}{b}\right)_k^2 = \frac{1 + \sqrt{(|\vec{\alpha}_k|^2 - |\vec{\beta}_k|^2)^2 + 4(\vec{\alpha}_k \cdot \vec{\beta}_k)^2}}{1 - \sqrt{(|\vec{\alpha}_k|^2 - |\vec{\beta}_k|^2)^2 + 4(\vec{\alpha}_k \cdot \vec{\beta}_k)^2}}$$

$$(30) \quad i_k = \arccos \hat{z} \cdot \hat{h}_k$$

$$(31) \quad \Omega_k = \arctan \frac{n_{y_k}}{n_{x_k}}$$

$$(32) \quad \psi_k = \arctan \frac{\mathbf{r}_k(\theta_\perp) \cdot \hat{t}_k}{\mathbf{r}_k(\theta_\perp) \cdot \hat{n}_k}$$

where \hat{n}_k is the ascending node vector and \hat{t}_k is its unit transverse vector, which can be obtained by the cross product of \hat{h}_k and \hat{n}_k .

Note that the above results are obtained for each mode $k = 1, 2, 3$. The true trajectory is the linear combination of all three modes. By understanding the behavior of each mode over an interval of time, we can sketch out the whole picture of the trajectory. These elements are osculating elements in that they vary slowly as a function of time. As we move through the halo orbit we are interested in observing the change in these elements, as this defines how the relative motion of the formation will be modified over time. Moreover, the mathematical formulae link the eigenvectors of the dynamic matrix with linear orbital elements, which converts the geometric distribution into the problem of eigenstructure properties.

TRAJECTORY DESIGN

In the previous section we defined sequences of linear orbit elements to understand the geometry of motion. Naturally, we are able to change the relative trajectories by adjusting those elements which are specified by the eigenstructures of $\tilde{A}(t_i)$ matrix. Thus, the design of relative motion is controlled by the matrix $\tilde{A}(t_i)$.

It is well known that for a controllable system we can arbitrarily place its poles ¹³. However, the desired closed-loop eigenvalues and eigenvectors may not be attainable at the same time since this is an overconstrained problem. This implies that closed-loop right eigenvectors cannot be assigned arbitrarily, and only those that belong to the span of the corresponding allowable subspace can be assigned precisely ¹⁴. Most people deal with this sort of problem with the technique of optimization, such as Ref. [14] and Ref. [15], either output feedback or state feedback. This algorithm tries to “rotate” the subspace of eigenstructures such that the weighting is minimum. With certain constraints the system must also satisfy, stability can then be guaranteed.

It is indeed a very useful tool for a regular control problem which requires poles on negative real plane. In our problem, however, these approaches are not applicable. Formation flight requires all closed-loop poles on the imaginary axis. Optimization of eigenvector placement might move those poles onto the real axis which would destabilized the formation dynamics. Therefore, we need to investigate other approaches to solve our unique problem.

Non-rotational System

To simplify the analysis we first consider a non-rotational system. By applying a controller to null out the Coriolis force and to stabilize system, we obtain the following equation of motion.

$$(33) \quad \delta \mathbf{r}'' - V(t)\delta \mathbf{r} = 0$$

Assume $V(t)$ is constant over a short time interval to derive the “instantaneous” motion. The characteristic equation is

$$(34) \quad \begin{aligned} \det(\omega^2 I - V) &= \det(M)\det(\omega^2 I - \Lambda_V)\det(M^{-1}) \\ &= \det(\omega^2 I - \Lambda_V) \\ &= (\omega^2 - \lambda_{v1})(\omega^2 - \lambda_{v2})(\omega^2 - \lambda_{v3}) \\ &= 0 \end{aligned}$$

where M is the eigenvector matrix and Λ_V is the diagonalized force potential. From linear theory, the force potential can be written as $V = M\Lambda_V M^{-1}$ and the eigenvectors satisfy the equation:

$$(35) \quad [\omega_i^2 I - V]\mathbf{v}_i = 0$$

Here we should note that the controlled V is negative definite so that $\lambda_{vi} < 0$. Then we can solve for this differential equation.

$$(36) \quad \delta \mathbf{r}(t) = \sum_{i=1}^3 \rho_i \mathbf{v}_i \cos(\sqrt{|\lambda_{vi}|}t + \phi_i)$$

where \mathbf{v}_i is the eigenvector for each mode; ρ_i and ϕ_i are determined by initial conditions. This equation tells us that, for each mode, the relative trajectory performs linear harmonic oscillations along the direction of eigenvectors with their associated eigenvalues as their frequencies. The real trajectory is just the linear combination of all three modes. Moreover, all the eigenvectors are orthonormal to each other because V is symmetric. That is, the eigenvector matrix M can be viewed as a rotation matrix. To generate a desired trajectory, we can initially assemble diagonal V matrix. Then choose a proper frequency ratio and initial conditions to generate a desired trajectory. Finally, apply frame rotation by pre- and post-multiplication by a rotation matrix to obtain a specific orientation.

Figures 10 and 11 show an example of mode combinations where a circular and an “8”-shaped trajectory are created. Having shown previously that the extra cost to eliminate Coriolis force is not very large, we have considerable freedom to perform trajectory design in this way.

Rotational System – Algebraic Approach

To understand the relationship between eigenvalues and eigenvectors, we need to look back at Eq. (20) in a 3DOF system. Assume $\pm jk_i$ are a pair of eigenvalue and $\tilde{\alpha}_i \pm j\tilde{\beta}_i$ are their associating eigenvectors. If we only apply a controller to the force potential, Eq. (20) can be expanded as

$$(37) \quad \begin{bmatrix} -k_i^2 - \bar{V}_{xx} & \mp 2k_i j - \bar{V}_{xy} & -\bar{V}_{xz} \\ \pm 2k_i j - \bar{V}_{xy} & -k_i^2 - \bar{V}_{yy} & -\bar{V}_{yz} \\ -\bar{V}_{xz} & -\bar{V}_{yz} & -k_i^2 - \bar{V}_{zz} \end{bmatrix} \begin{bmatrix} a_{1i} \pm j b_{1i} \\ a_{2i} \pm j b_{2i} \\ a_{3i} \pm j b_{3i} \end{bmatrix} = 0$$

And the characteristic equation would be

$$(38) \quad \det(-k_i^2 I - 2k_i j J - \bar{V}) = 0$$

where $\vec{\alpha}_i = (a_{1i}, a_{2i}, a_{3i})$, $\vec{\beta}_i = (b_{1i}, b_{2i}, b_{3i})$, $i = 1, 2, 3$ denote the i th mode, and \vec{V} denotes the normalized controlled force potential with respect to the rotation rate ω of the frame. Now we only consider one mode and rewrite Eq. (37) as a function of \vec{V}_{ij} .

$$(39) \quad \begin{bmatrix} a_1 & a_2 & a_3 & 0 & 0 & 0 \\ b_1 & b_2 & b_3 & 0 & 0 & 0 \\ 0 & a_1 & 0 & a_2 & a_3 & 0 \\ 0 & b_1 & 0 & b_2 & b_3 & 0 \\ 0 & 0 & a_1 & 0 & a_2 & a_3 \\ 0 & 0 & b_1 & 0 & b_2 & b_3 \end{bmatrix} \begin{bmatrix} \vec{V}_{xx} \\ \vec{V}_{xy} \\ \vec{V}_{xz} \\ \vec{V}_{yy} \\ \vec{V}_{yz} \\ \vec{V}_{zz} \end{bmatrix} = -k^2 \begin{bmatrix} a_1 \\ b_1 \\ a_2 \\ b_2 \\ a_3 \\ b_3 \end{bmatrix} - 2k \begin{bmatrix} -b_2 \\ a_2 \\ b_1 \\ -a_1 \\ 0 \\ 0 \end{bmatrix}$$

Or in the form of $\mathbf{P}_i \vec{V} = \mathbf{Q}_i(\vec{V})$, $i = 1, 2, 3$. Since all the three modes have to satisfy the same force potential, Eq. (39) are valid for all the three modes. Let

$$(40) \quad \mathbf{P} = \begin{bmatrix} \mathbf{P}_1 \\ \mathbf{P}_2 \\ \mathbf{P}_3 \end{bmatrix}$$

$$(41) \quad \mathbf{Q} = \begin{bmatrix} \mathbf{Q}_1 \\ \mathbf{Q}_2 \\ \mathbf{Q}_3 \end{bmatrix}$$

Then we can combine those three modes and write as $\mathbf{P} \vec{V} = \mathbf{Q}(\vec{V})$, where $\mathbf{P} \in \mathbb{R}^{18 \times 6}$ and $\mathbf{Q} \in \mathbb{R}^{18}$. It is an overconstraint simultaneous nonlinear equations with 6 unknowns and 18 equations. The solution exists *if and only if* $\mathbf{Q}(\vec{V}) \in \mathcal{RA}\{\mathbf{P}\}$. We should note that both \mathbf{P} and \mathbf{Q} are functions of k , $\vec{\alpha}$ and $\vec{\beta}$, and k in turn is also a function of \vec{V} . Generally speaking, this problem is difficult to solve.

In a practical issue, we can pick a set of candidate eigenvectors and eigenvalues, and plug them into Eqs. (38) and (39) to see if they satisfy both equations. Since we have more constraints if we consider all three modes at the same time, one way to simplify the situation is to only specify one mode and let the other two modes be free. Upon finding some candidate force potentials, we can then pick the negative definite ones so that the stability is guaranteed.

Application to A Specific Case

The most specific case is to design a circular relative trajectory. As our design method above, we only consider one mode here and pick the negative force potential at the end. From Eqs.(27) and (29), we can conclude that $\vec{\alpha} \perp \vec{\beta} \perp \hat{h}$ and $|\vec{\alpha}| = |\vec{\beta}| = 1/\sqrt{2}$ for a circular trajectory mode. Assume $\vec{\alpha} = (\hat{a}_1, \hat{a}_2, \hat{a}_3)/\sqrt{2}$, $\vec{\beta} = (\hat{b}_1, \hat{b}_2, \hat{b}_3)/\sqrt{2}$ and $\hat{h} = (h_1, h_2, h_3)$, where \hat{a}_i and \hat{b}_i denotes the unit vector components of $\vec{\alpha}$ and $\vec{\beta}$. Then $\hat{h} = 2(\vec{\beta} \times \vec{\alpha})$. Accordingly,

$$\begin{aligned} \hat{a} &= \hat{h} \times \hat{\beta} \\ &= \begin{bmatrix} h_2 \hat{b}_3 - h_3 \hat{b}_2 \\ h_3 \hat{b}_1 - h_1 \hat{b}_3 \\ h_1 \hat{b}_2 - h_2 \hat{b}_1 \end{bmatrix} \\ \hat{\beta} &= \hat{a} \times \hat{h} \\ &= \begin{bmatrix} -h_2 \hat{a}_3 + h_3 \hat{a}_2 \\ -h_3 \hat{a}_1 + h_1 \hat{a}_3 \\ -h_1 \hat{a}_2 + h_2 \hat{a}_1 \end{bmatrix} \end{aligned}$$

Plug it into Eq. (39) and perform some algebraic manipulation to find two relations.

$$(42) \quad \begin{bmatrix} k^2 + 2kh_3 + \vec{V}_{xx} & \vec{V}_{xy} & -2kh_1 + \vec{V}_{xz} \\ \vec{V}_{xy} & k^2 + 2kh_3 + \vec{V}_{yy} & -2kh_2 + \vec{V}_{yz} \\ \vec{V}_{xz} & \vec{V}_{yz} & k^2 + \vec{V}_{zz} \end{bmatrix} \vec{\alpha} = 0$$

$$(43) \quad N\vec{\alpha} = 0$$

where

$$\begin{aligned}
N_{11} &= -\bar{V}_{xy}h_3 + \bar{V}_{xz}h_2 \\
N_{12} &= (k^2 + \bar{V}_{xx})h_3 - \bar{V}_{xz}h_1 + 2k \\
N_{13} &= -(k^2 + \bar{V}_{xx})h_2 + \bar{V}_{xy}h_1 \\
N_{21} &= -(k^2 + \bar{V}_{yy})h_3 + \bar{V}_{yz}h_2 - 2k \\
N_{22} &= \bar{V}_{xy}h_3 - \bar{V}_{yz}h_1 \\
N_{23} &= -\bar{V}_{xy}h_2 + (k^2 + \bar{V}_{yy})h_1 \\
N_{31} &= -\bar{V}_{yz}h_3 + (k^2 + \bar{V}_{zz})h_2 \\
N_{32} &= \bar{V}_{xz}h_3 - (k^2 + \bar{V}_{zz})h_1 \\
N_{33} &= -\bar{V}_{xz}h_2 + \bar{V}_{yz}h_1
\end{aligned}$$

Note that $\vec{\beta}$ also has to satisfy Eqs. (42) and (43). Since $\vec{\alpha}$ is perpendicular to $\vec{\beta}$, the rank of Eqs. (42) and (43) cannot be greater than one, and $\vec{\alpha}$ and $\vec{\beta}$ must be located in the null space of both matrices.

Consider a specific case in which the off diagonal terms in \bar{V} are all zero. Then Eqs. (42) and (43) simplify to

$$(44) \quad \begin{vmatrix} k^2 + 2kh_3 + \bar{V}_{xx} & 0 & -2kh_1 \\ 0 & k^2 + 2kh_3 + \bar{V}_{yy} & -2kh_2 \\ 0 & 0 & k^2 + \bar{V}_{zz} \end{vmatrix} = 0$$

$$(45) \quad \begin{vmatrix} 0 & (k^2 + \bar{V}_{xx})h_3 + 2k & -(k^2 + \bar{V}_{xx})h_2 \\ -(k^2 + \bar{V}_{yy})h_3 - 2k & 0 & (k^2 + \bar{V}_{yy})h_1 \\ (k^2 + \bar{V}_{zz})h_2 & -(k^2 + \bar{V}_{zz})h_1 & 0 \end{vmatrix} = 0$$

The expansion of Eq. (45) is

$$(46) \quad 2h_1h_2k(k^2 + \bar{V}_{zz})(-\bar{V}_{xx} + \bar{V}_{xx}) = 0$$

one of the possible solutions in Eq. (46) is $k^2 + \bar{V}_{zz} = 0$, which is consistent with Eq. (44). Since we know the rank of Eqs. (44) and (45) are not greater than one, this is not a qualified solution. The other one solution is $\bar{V}_{xx} = \bar{V}_{yy}$, and, from Eq. (44), we conclude that $\bar{V}_{xx} = \bar{V}_{yy} = -(k^2 + 2kh_3)$. Therefore, $\hat{\beta} = (1, 0, 0)$, $\hat{\alpha} = (0, 1, 0)$ and $\hat{h} = (0, 0, 1)$. On the other hand, $-k^2 = \bar{V}_{xx} + 2k = \bar{V}_{yy} + 2k$. We find that the characteristic equation, Eq. (38), is also satisfied. Moreover, Eqs. (44) and (45) both degenerate to $rank \leq 1$ with these results. That shows the consistency in our derivation.

Rotational System – Geometric Approach

Augmented Matrix

Another approach to dealing with complex matrices is to form an augmented matrix in which the real part and imaginary part are included. The matrix in Eq. (37) is complex and this approach can be applied. Assume the eigenvectors are in the form $\mathbf{u} = \vec{\alpha} \pm j\vec{\beta}$. Without loss of generality, we only take the “plus sign” into consideration. Re-write Eq. (37) as

$$(47) \quad \begin{aligned} (\mathcal{A} + j\mathcal{B})(\vec{\alpha} + j\vec{\beta}) &= 0 \\ \mathcal{A} &= -k^2I - \bar{V} \\ \mathcal{B} &= -2kJ \end{aligned}$$

where \mathcal{A} is symmetric and \mathcal{B} is skew symmetric. Thus, a linear equation of augmented real block matrices is established.

$$(48) \quad \mathcal{A}\vec{\alpha} - \mathcal{B}\vec{\beta} = 0$$

$$(49) \quad \mathcal{A}\vec{\beta} + \mathcal{B}\vec{\alpha} = 0$$

Taking inner product of Eq. (48) with $\vec{\alpha}$ and Eq. (49) with $\vec{\beta}$, we obtain,

$$(50) \quad \vec{\alpha}^T \mathcal{A} \vec{\alpha} = \vec{\alpha}^T \mathcal{B} \vec{\beta}$$

$$(51) \quad \vec{\beta}^T \mathcal{A} \vec{\beta} = -\vec{\beta}^T \mathcal{B} \vec{\alpha}$$

However, Eq. (50) and Eq. (51) can be expanded as $\vec{\alpha}^T \mathcal{B} \vec{\beta} = -\vec{\beta}^T \mathcal{B} \vec{\alpha} = 2kH_3$, where H_3 is the third component of $\vec{\beta} \times \vec{\alpha}$, the ‘‘linear angular momentum’’, and is a scalar. If $H_3 \neq 0$, Eqs. (50) and (51) can be reformed as

$$(52) \quad \vec{\alpha}^T \left(\frac{1}{2kH_3} \mathcal{A} \right) \vec{\alpha} = 1$$

$$(53) \quad \vec{\beta}^T \left(\frac{1}{2kH_3} \mathcal{A} \right) \vec{\beta} = 1$$

Geometric Interpretation

The geometric interpretation of an equation of the form $X^T A X = 1$ is an conoid in three dimensional space, where X is a vector and A is an 3 by 3 matrix. The principle axes of this conoid lie along with the eigenvectors of matrix A , and the size as well as the shape of this conoid is determined by the eigenvalues of matrix A . The expansion of the quadratic equation $X^T A X = 1$ usually contains all combination of x , y and z . However, with proper choice of bases, or coordinate rotation in the geometric viewpoint, we can get a very neat expression. Assume λ_1 , λ_2 and λ_3 are eigenvalues of A . Under a specific set of bases we obtain,

$$(54) \quad \begin{aligned} X^T A X &= \lambda_1 x^2 + \lambda_2 y^2 + \lambda_3 z^2 \\ &= \pm \frac{x^2}{a^2} \pm \frac{y^2}{b^2} \pm \frac{z^2}{c^2} \\ &= 1 \end{aligned}$$

where the choice of sign depends on the signs of λ 's. The geometric shapes of Eq. (54) are classified into seventeen groups¹⁶. As a result, in our case, $a^2 = 2kH_3/(k_i^2 - \lambda_j)$, where i denotes the i th mode of whole system and j denotes the j th eigenvalue of \vec{V} . Similarly, b^2 and c^2 has the same form but different values.

It's obvious that Eq. (52) and Eq. (53) have similar structure. Moreover, since the force potential \vec{V} is symmetric, its eigenvector matrix can be chosen orthonormal. Assume M is the orthonormal eigenvector matrix, so that $M^{-1} = M^T$ and $\vec{V} = M \Lambda_{\vec{V}} M^T$, where $\Lambda_{\vec{V}}$ is the diagonalized force potential. Then,

$$(55) \quad \begin{aligned} \frac{1}{2kH_3} \mathcal{A} &= \frac{1}{2kH_3} (-k^2 I - \vec{V}) \\ &= M \left[\frac{1}{2kH_3} (-k^2 I - \Lambda_{\vec{V}}) \right] M^T \end{aligned}$$

Eq. (55) shows that matrix \mathcal{A} has the same eigenvector as \vec{V} . That is, the conoid formed by matrix \mathcal{A} has the same orientation as that formed by \vec{V} . Nevertheless, it has a different size and shape and is either an ellipsoid or a hyperboloid. The shape and size are determined by the relationship between k and eigenvalues of \vec{V} .

The above analysis tells us that both $\vec{\alpha}$ and $\vec{\beta}$ must lie on the surface of the conoid. On the other hand, $\vec{\alpha}$ and $\vec{\beta}$ also form the orbital plane. Consequently, $\vec{\alpha}$ and $\vec{\beta}$ must lie on the intersecting ellipse or hyperbola, as depicted in Figure (12). This instead limits the choice of orientation of an orbital plane, which is consistent with our previous conclusion. This idea may help us to analyze or design a trajectory from the viewpoint of geometry.

Application to A Specific Case

To design a trajectory by choosing eigenvectors, we must constrain $\vec{\alpha}$ and $\vec{\beta}$ to lie on the intersecting curve of a conoid and the desired orbital plane. One of the specific cases is to place the orbit plane on the one formed by \mathbf{e}_1 and \mathbf{e}_2 , any two eigenvectors of the force potential. By choosing these eigenvectors, it may be possible for us to orient the orbit plane in a specific attitude. Specifically, let

$$\begin{aligned}
 \vec{\alpha} &= \alpha_1 \mathbf{e}_1 + \alpha_2 \mathbf{e}_2 \\
 \vec{\beta} &= \beta_1 \mathbf{e}_1 + \beta_2 \mathbf{e}_2 \\
 M &= \begin{bmatrix} \mathbf{e}_1 & \mathbf{e}_2 & \mathbf{e}_3 \end{bmatrix} \\
 (56) \quad &= \begin{bmatrix} e_{11} & e_{12} & e_{13} \\ e_{21} & e_{22} & e_{23} \\ e_{31} & e_{32} & e_{33} \end{bmatrix}
 \end{aligned}$$

where M is the orthonormal eigenvector matrix of $\bar{\mathbf{V}}$. Substitute into Eq. (48) and Eq. (49) and after a few algebraic manipulations (Appendix I), we can show that the plane normal to the Z-axis is the only solution. Actually, this result can also be obtained by directly solving for the equations of motion, which gives us a more dynamical interpretation of this phenomenon.

First we can express the force potential in terms of its eigenvalues and eigenvectors.

$$(57) \quad \mathbf{V} = [\lambda_1 \mathbf{e}_1 \mathbf{e}_1^T + \lambda_2 \mathbf{e}_2 \mathbf{e}_2^T + \lambda_3 \mathbf{e}_3 \mathbf{e}_3^T]$$

Assume the orbit plane lies on the \mathbf{e}_1 - \mathbf{e}_2 plane. The trajectory, $\mathbf{r}(t)$, can be written as the linear combination of these two eigenvectors

$$\begin{aligned}
 \mathbf{r}(t) &= r_1(t) \mathbf{e}_1 + r_2(t) \mathbf{e}_2 \\
 \dot{\mathbf{r}}(t) &= \dot{r}_1(t) \mathbf{e}_1 + \dot{r}_2(t) \mathbf{e}_2 \\
 \ddot{\mathbf{r}}(t) &= \ddot{r}_1(t) \mathbf{e}_1 + \ddot{r}_2(t) \mathbf{e}_2
 \end{aligned}$$

Plug into the equations of motion

$$\ddot{\mathbf{r}}(t) = 2\omega J \dot{\mathbf{r}}(t) + V \mathbf{r}(t)$$

Consider the Z-component to this equation,

$$\begin{aligned}
 \ddot{r}_1(t) e_{31} &= \lambda_1 e_{31} r_1(t) \\
 \ddot{r}_2(t) e_{32} &= \lambda_2 e_{32} r_2(t)
 \end{aligned}$$

Since $\lambda_1 < 0$ and $\lambda_2 < 0$, if e_{31} and e_{32} are not zero, the solutions would be

$$\begin{aligned}
 r_1(t) &= \rho_1 \cos(\sqrt{|\lambda_1|} t) \\
 r_2(t) &= \rho_2 \cos(\sqrt{|\lambda_2|} t)
 \end{aligned}$$

However, these don't satisfy the differential equations in the X and Y components because the Coriolis force will slightly change the system frequency. So, we can't find an oscillating frequency which makes the trajectory remain on the \mathbf{e}_1 - \mathbf{e}_2 plane if we have Z component. Namely, the only possibility is that the orbit remains on the XY plane.

CONCLUSIONS

In this paper we analyze the dynamics of motion relative to an unstable periodic orbit. We first consider general equations of motion and try to find a sufficient condition under which the relative motions are stable. Then, based on previous work on linear orbital elements, we develop different algorithms for trajectory design. This work is being developed for future application to spacecraft-based interferometric imaging located in the vicinity of the Earth-Sun L_2 libration point.

ACKNOWLEDGEMENTS

The work described here was funded in part by NASA's Office of Space Science and by the Interplanetary Network Technology Program by a grant from the Jet Propulsion Laboratory, California Institute of Technology which is under contract with the National Aeronautics and Space Administration.

APPENDIX I

Let $\mathbf{e}_1, \mathbf{e}_2, \mathbf{e}_3$ be the orthonormal eigenvectors of $\bar{\mathbf{V}}$ matrix and $\lambda_1, \lambda_2, \lambda_3$ be the corresponding eigenvalues. Assume $\vec{\alpha}$ and $\vec{\beta}$ are located on the plane formed by any two eigenvectors. Without loss of generality, the \mathbf{e}_1 - \mathbf{e}_2 plane is chosen. Then

$$(58) \quad \vec{\alpha} = \alpha_1 \mathbf{e}_1 + \alpha_2 \mathbf{e}_2$$

$$(59) \quad \vec{\beta} = \beta_1 \mathbf{e}_1 + \beta_2 \mathbf{e}_2$$

$$\begin{aligned} \mathcal{A} &= -k^2 I - \bar{\mathbf{V}} \\ &= M(-k^2 I - \Lambda_{\bar{\mathbf{V}}})M^T \\ &= \left[(-k^2 - \lambda_1) \mathbf{e}_1 \mathbf{e}_1^T + (-k^2 - \lambda_2) \mathbf{e}_2 \mathbf{e}_2^T + (-k^2 - \lambda_3) \mathbf{e}_3 \mathbf{e}_3^T \right] \end{aligned}$$

Plug Eqs.(58) and (59) into Eqs.(48) and (49) to obtain

$$(60) \quad \alpha_1(-k^2 - \lambda_1) \mathbf{e}_1 + \alpha_2(-k^2 - \lambda_2) \mathbf{e}_2 = 2J(\beta_1 \mathbf{e}_1 + \beta_2 \mathbf{e}_2)$$

$$(61) \quad \beta_1(-k^2 - \lambda_1) \mathbf{e}_1 + \beta_2(-k^2 - \lambda_2) \mathbf{e}_2 = -2J(\alpha_1 \mathbf{e}_1 + \alpha_2 \mathbf{e}_2)$$

Consider the third components of Eqs. (60) and (61), we can conclude that

$$\begin{aligned} \alpha_1(-k^2 - \lambda_1) e_{31} + \alpha_2(-k^2 - \lambda_2) e_{32} &= 0 \\ \beta_1(-k^2 - \lambda_1) e_{31} + \beta_2(-k^2 - \lambda_2) e_{32} &= 0 \end{aligned}$$

Or in matrix form

$$(62) \quad \begin{bmatrix} \alpha_1 & \alpha_2 \\ \beta_1 & \beta_2 \end{bmatrix} \begin{bmatrix} p \\ q \end{bmatrix} = 0$$

where $p = (-k^2 - \lambda_1) e_{31}$ and $q = (-k^2 - \lambda_2) e_{32}$. Since $\vec{\alpha}$ is not parallel to $\vec{\beta}$, the matrix is full rank. Therefore, $[p \ q]^T = 0$. Moreover, due to the Coriolis term in the characteristic equation, the system eigenvalues, $-k_i^2$, are not equal to the eigenvalues of force potential, λ_j . Hence, the only solution to Eq. (62) is $e_{31} = e_{32} = 0$, i.e., $\mathbf{e}_3 = (0, 0, 1)$.

REFERENCES

- 1 Barden, B.T. and K.C. Howell, "Fundamental Motions Near Collinear Libration Points and Their Transitions", *Journal of the Astronautical Sciences*, Vol. 46, 1998, pp. 361–378
- 2 Howell, K.C., B.T. Barden, M.W. Lo, "Application of Dynamical Systems Theory to Trajectory Design for a Libration Point Mission", *J. of the Astronautical Sciences*, Vol. 45, 161–178, 1997
- 3 Gómez, G., J. Masdemont, and C. Simo, "Quasihalo Orbits Associated with Libration Points", *Journal of the Astronautical Sciences*, Vol. 46, 1998, pp. 135–176
- 4 Schaub, H. and K.T. Alfriend, "Impulsive Feedback Control to Establish Specific Mean Orbit Elements of Spacecraft Formations", *Journal of Guidance, Control and Dynamics*, Vol. 24, No. 4, 2001, pp. 739–745
- 5 Mesbahi, M. and F.Y. Hadaegh, "Formation Flying Control of Multiple Spacecraft via Graphs, Matrix Inequalities, and Switching", *Journal of Guidance, Control and Dynamics*, Vol. 24, No. 2, 2001, pp. 369–377
- 6 Sabol, C., R. Burns, and C.A. McLaughlin, "Satellite Formation Flying Design and Evolution", *Journal of Spacecraft and Rockets*, Vol. 38, No. 2, 2001, pp. 270–278
- 7 Hussen, I., D.J. Scheeres and D.C. Hyland, "Interferometric Observatories in Low Earth Orbit", submitted to *Journal of Guidance, Control and Dynamics*
- 8 Marchal, C., *The Three-Body Problem*, Elsevier, 1990, pp. 64
- 9 Scheeres, D.J., F.Y. Hsiao and N.X. Vinh, "Stabilizing Motion Relative to An Unstable Orbit: Applications to Spacecraft Formation Flight", *Journal of Guidance, Control and Dynamics* accepted
- 10 Hsiao, F.Y. and D.J. Scheeres, "The Dynamics of Formation Flight About a Stable Trajectory", *AAS Paper 02-189*
- 11 Nemytskii V. V, V.V. Stepanov, *Qualitative Theory of Differential Equations*, Dover, 1989, pp. 152
- 12 Bate, R.R, Mueller D.D., White, J.E., *Fundamentals of Astrodynamics*, Dover, New York, 1971, pp. 58–63
- 13 Bay, J.S., *Fundamentals of Linear State Space systems*, 1999, pp. 419
- 14 Liu, G.P., R.J. Patton, *Eigenstructure Assignment for Control System Design*, 1998, pp. 20
- 15 Subrahmanyam, P., D. Trumper, "Eigenvector Assignment", 1999 AACC
- 16 Zwillinger, D., *CRC Standard Mathematical Tables And Formulae*, 30th Edition, pp. 316 – 319

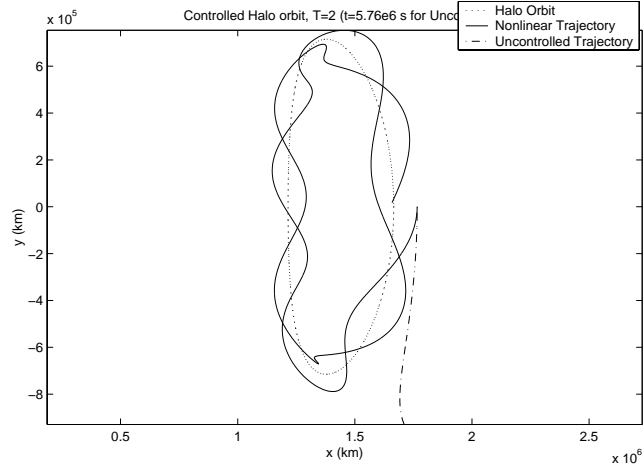


Figure 1: A control law $\mathcal{T}_c = -\sigma^2 G[u_+ u_+^T + u_- u_-^T]$ with $G = 10$ is applied (Eq. (26)) Initial deviation is 1×10^5 km in x-direction. This plot shows the stability in a nonlinear version.

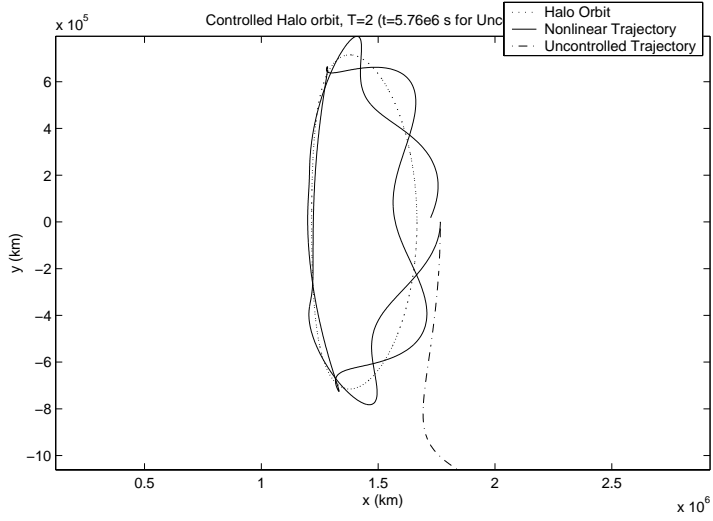


Figure 2: A desired force potential $\tilde{V}_{rr} = -2.7 \times 10^{-12} I_{3 \times 3}$ is chosen and the controller is $\mathcal{T}_c = -(\tilde{V}_{rr} - V_{rr})\delta\mathbf{r}$. Initial deviation is 1×10^5 km in x-direction. This plot shows the stability in a nonlinear version.

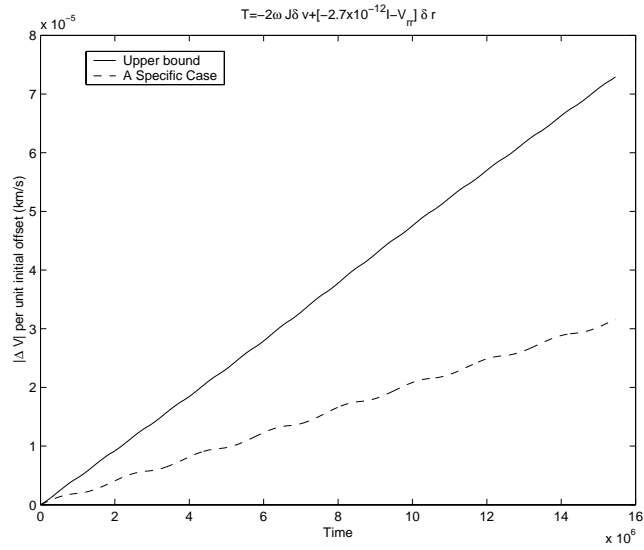


Figure 3: The first figure shows that the upper bound on total cost per unit initial offset to create a non-Coriolis system, and the cost of a specific example with $r_0 = 1$ km.

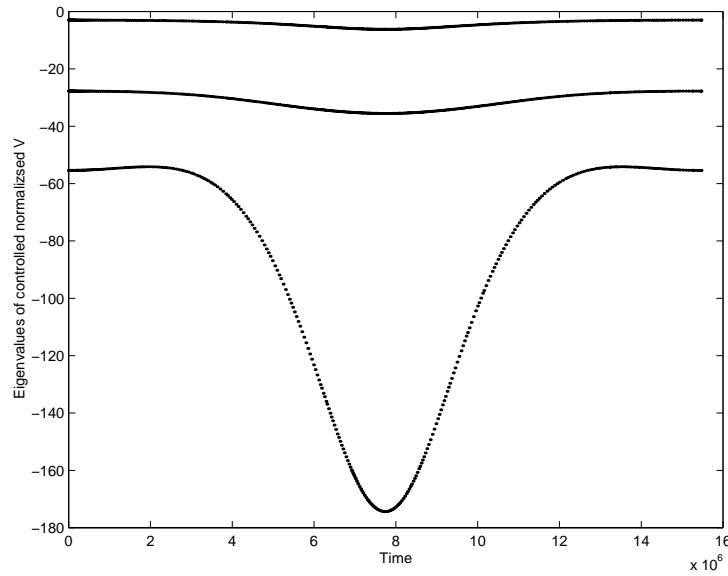


Figure 4: Eigenvalues of control law in Eq. (26). We see that the V is negative definite

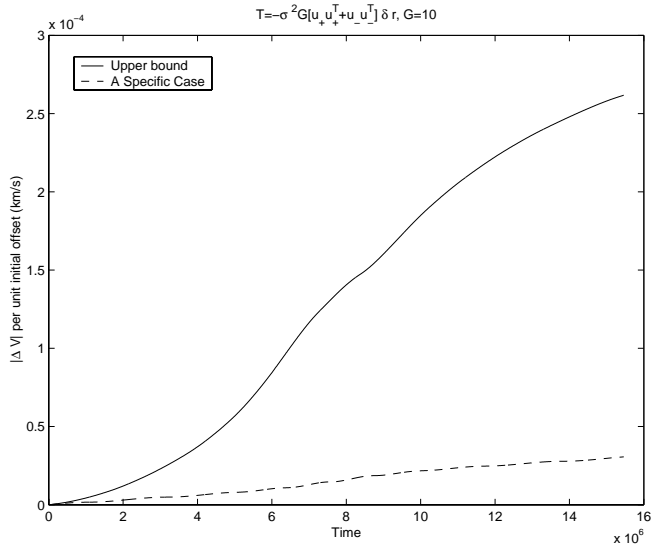


Figure 5: The first figure shows that the upper bound on total cost per unit initial offset as we apply the controller $T = -\sigma^2 G[\mathbf{u}_+ \mathbf{u}_+^T + \mathbf{u}_- \mathbf{u}_-^T]$ and $G = 10$, and the cost of a specific example with $r_0 = 1$ km.

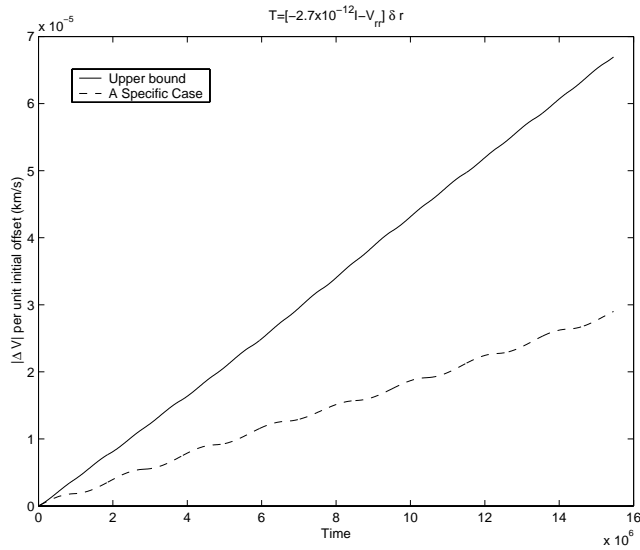


Figure 6: The first figure shows that the upper bound on total cost per unit initial offset to create circular trajectory with constant frequency over an entire period, and the cost of a specific example with $r_0 = 1$ km.

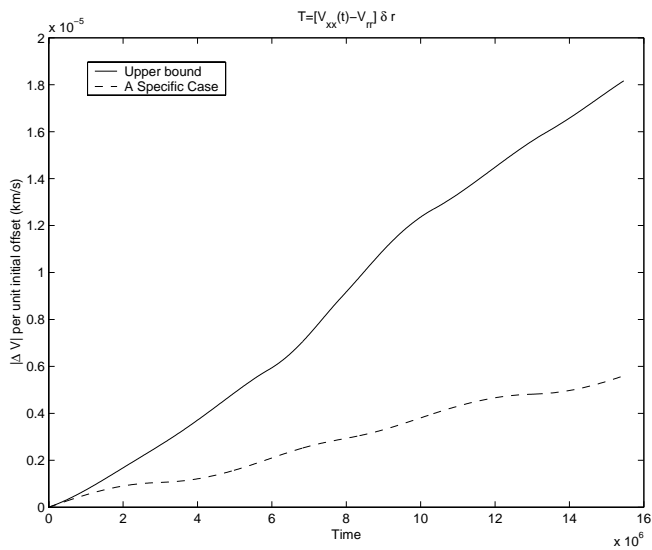


Figure 7: The first figure shows that the upper limit of total cost per unit initial offset in order to create circular trajectory with varying frequency over a whole period. The second figure gives the actual cost when $r_0 = 1$ km.

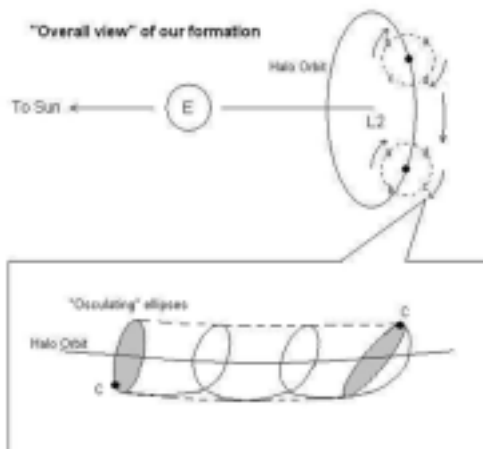


Figure 8: An overall view of the formation flight of spacecraft and how “osculating” ellipses describe relative linear trajectories.

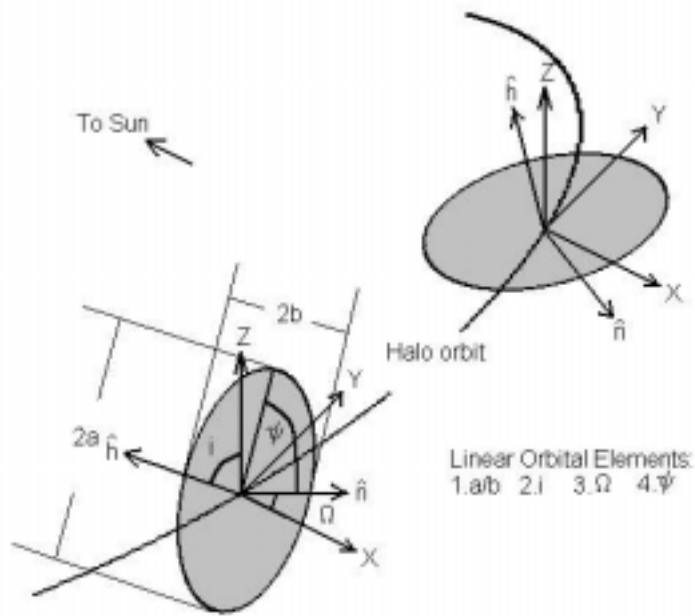


Figure 9: The definition of the “Linear Orbital Elements”.

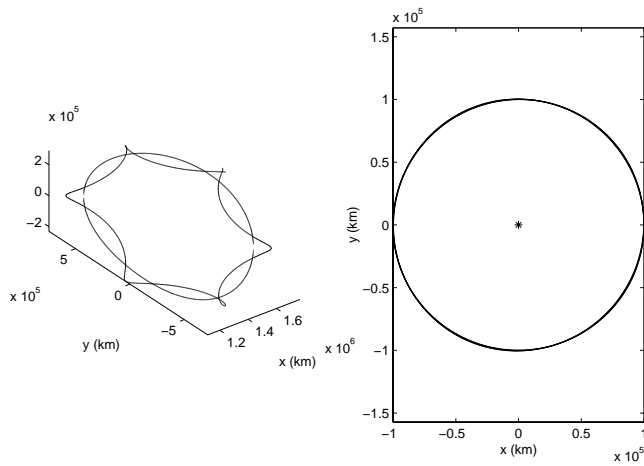


Figure 10: A relative circular trajectory is created in a non-Coriolis system. (a) Integrated in the original non-linear equations about a halo orbit. (b) Same Orbit relative to the halo orbit in (a)

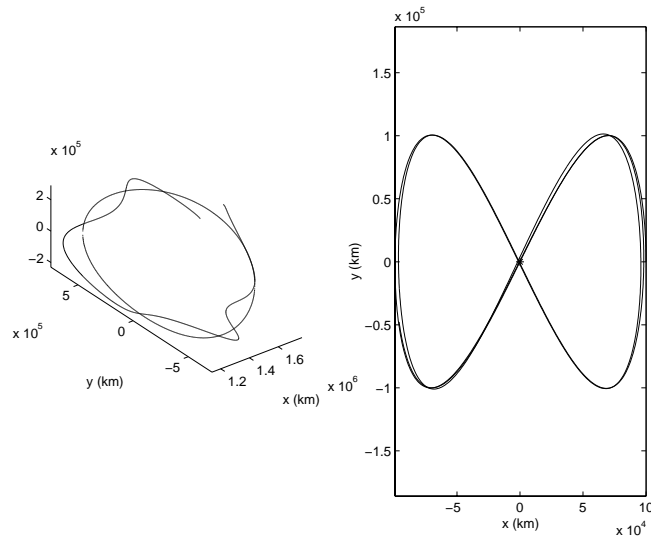


Figure 11: A relative figure-“8” trajectory in a non-Coriolis system. (a) Integrated in the original non-linear equations about a halo orbit. (b) Same Orbit relative to the halo orbit in (a)

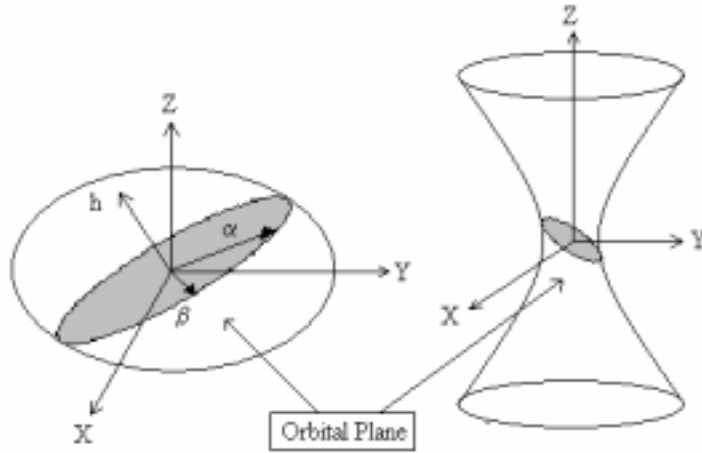


Figure 12: The Geometric Approach and the relationship between eigenvectors and conoids. $\vec{\alpha}$ and $\vec{\beta}$ denote the real and imaginary part of an eigenvector in our controlled system, respectively.